Proceedings of the 2009 IEEE
International Conference on Robotics and Biomimetics
December 19 -23, 2009, Guilin, China

Two-Phased Force and Coordinates Controller for a Pair of 2-DOF Soft Fingers

Yujiro Yamazaki, Takaihro Inoue and Shinichi Hirai

***Abstract*— We have previously shown that a hemispherical soft fingertip is in equilibrium when it is in contact with an object. The characteristics of the contact force and flexibility of a soft fingertip are important in stable grasping and manipulation. Hence, using these characteristics soft fingers can manipulate objects dexterously. We previously focused on a pair of 1-DOF fingers with soft fingertips. In this paper, we present a control scheme by which a pair of 2-DOF soft fingers can control a grasped object's planar coordinates. First, we formulate the equations of motion of soft fingered manipulation, which has the local minimum of elastic potential energy (LMEE), defined as the characteristic of equilibrium that appear during manipulation. Next, we propose a new control scheme, which can control a grasped object's planar coordinates. The proposed control scheme includes a positional controller of each finger joint angle and an integral controller of the object coordinates. Finally, we apply this control scheme to an experiment and a simulation, based on a parallel distributed virtual spring model to control planar coordinates of a grasped object. The agreement between our experimental and simulated results shows the validity of our control scheme. At the end of the paper, we show the possibility of controlling the grasping force by extending the theory of the proposed controller.**

I. INTRODUCTION

Soft fingertips can stably grasp an object relatively easily, because the soft material adaptively deforms along the surface of the grasped object. Precise control is harder to accomplish by soft fingers than by hard fingers. The phenomena in hard finger manipulation can be easily derived by kinematics. In soft finger manipulation, In contrast, the nonlinear behavior of the soft material affects model based control. As a result of the accumulation of errors caused during manipulation, the manipulation task can fail. Without making a proper model of soft fingers and of a control scheme, precise manipulation cannot be realized. Before introducing our new control scheme, we describe the history of soft fingered robotic hands, in terms of their control schemes.

The first soft fingered robotic hand was proposed by Hanafusa and Asada [1], [2]. They found that the optimal prehension strategy can be derived by computing the local minimum elastic energy induced on the elastic components of soft fingers. However, while describing their prehension strategy, they did not describe manipulations after grasping an object. Later researches involved actual soft finger manipulations.

More recently, realistic models of soft fingers have been described. Arimoto *et al*. proposed a mathematical model in which the elastic force of a soft fingertip can be derived by solving equations for the elastic force caused by the deformation of an elastic spherical cone [3]. This model was successful in realizing the nonlinear function of the elastic force of a soft fingertip. Furthermore, based on this model, Doulgeri *et al*. proposed a feedback controller designed to control an object's two coordinates and internal force with a pair of 2-DOF soft fingers [4], [5]. However, their control scheme was based on a hard contact mechanism. Furthermore, this model did not include an angle dependent characteristic of soft finger elasticity. Hence, precise control with an actual soft fingered hand is difficult to accomplish.

Inoue *et al*. previously reported that LMEE was an intrinsic characteristic of hemispherical soft fingertips [6], [7], [8]. This characteristic indicates that the induced elastic potential energy is dependent on the angle of contact surface, and that it is in equilibrium when the angle of the contact surface is zero. This equilibrium was present even during soft finger manipulation, and this group proposed a controller that does not need a Jacobian matrix or a complicated mathematical model [9], [10]. Their controller is composed of an integral controller, for generating the desired angle of joints, and a KP controller of joint angle. Thus, their controller can control object posture in the absence of a unique desired joint angle. That is, the desired angle of a finger joint can be adapted to the current object posture. Interestingly, the grasping force term in their model was independent. Hence, by extending their theory, we can design a controller that can control not only the orientation of an object, but also the grasping force. Five joints on robotic hands are believed to be able to control four DOFs of an object. However, by extending the proposed controller Inoue *et al*., we can design a controller by which a pair of 2-DOF soft fingers can control three coordinates of an object and the grasping force (Fig. 1).

In this paper, we start by describing the dynamic model of a pair of 2-DOF soft fingers and a new controller. We then apply the new controller to the soft fingered hand to control an object's three coordinates. To determine the validity of this control, we apply it to an actual soft fingered hand. At the end of the paper, we show that introducing feedback to the proposed control may enable the control of the grasping force.

This work was supported in part by JSPS Crant in Aid for Scientific Research No. 20246094.

Y. Yamazaki is with Graduate school of Science Engineering, Robotics, Ritsumeikan University, 1-1-1 Nojihigashi, Kusatsu, Japan rr007044@ed.ritsumei.ac.jp

T. Inoue is with Department of System Engineering for Sports, Okayama Prefectural University, Japan inoue@ss.oka-pu.ac.jp

S. Hirai is with Faculty of the Depertment of Robotics, Ritsumeikan University, Japan hirai@se.ritsumei.ac.jp

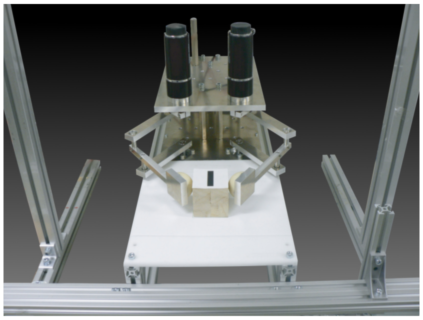

Fig. 1. A Pair of 2 DOFs Soft Fingered Robotic Hand

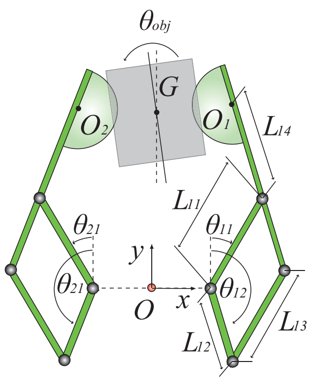

Fig. 2. System of Soft Fingered Manipulation

II. EQUATIONS OF MOTION OF A TWO-FINGERED HAND WITH SOFT TIPS

In this section, we derive equations of motion of object manipulation performed by two 2-DOF robotic fingers with soft fingertips driven by a parallel link mechanism (Fig. 2). The manipulation area was limited to a 2D plane. We employ a parallel distributed model [7], [8], which includes not only the nonlinear function of soft fingertip elasticity but also an angle dependent elasticity function which was not included in the model proposed by Arimoto *et al*. [3]. We assumed that the two soft fingers and the grasped object form a closed link mechanism without any slippage between the soft fingertips and the object. We therefore introduced four geometric constraints. Two of these are holonomic constraints that generate normal constraints on the object surface and the fingertips. The others are nonholonomic constraints that generate tangential constraints on the object and fingertips. In this section we start by explaining the four constraints. We then explain our parallel distributed model, its kinetic energy and its equations of motion. Because the gravity acts in the negative direction of z-axis in Fig. 2, we can ignore the gravitational term when deriving equations of motion. Finally, we introduce a numerical solution to simulate soft fingered manipulation.

A. Holonomic and Nonholonomic Constraints

Let the right finger be the first finger and the left finger be the second finger. In the equations above, let (x_{obj}, y_{obj}) be the position of a grasped object, θ_{obj} be the tilt, a the radius

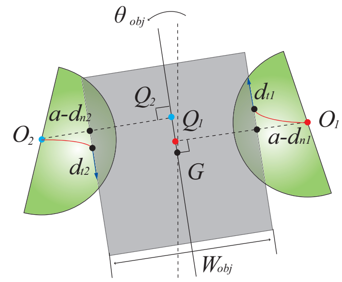

Fig. 3. Fingertips and an Object

of the soft fingertips, d_{ni} the deformation of the i-th fingertip, which is perpendicular to the surface of the object, and W_{obj} the width of the object. Let $2W_{fi}$ be the distance of the base coordinates of two soft fingers, w the distance between the center of the object and COG in the normal direction and L_{ij} the length of the i-th finger's j-th link. Thus, subscript i stands for the i-th finger and subscript j for the j-th link. Let θ_{ij} be each joint angle. The positive rotation of first finger is counterclockwise, and the positive rotation of the second finger is clockwise. Let $2d_{fi}$ be the thickness of the links of the fingers. Equations (2) and (3) thus describe the position of the center of the i-th fingertip. The two holonimoc constraints are represented by the geometric relationship of the i-th fingertip and the surface of object as:

$$\begin{aligned} C_i^H \;=\; & (-1)^i (x_{obj} - O_{ix}) \cos\theta_{obj} \\ & + (-1)^i (y_{obj} - O_{iy}) \sin\theta_{obj} \\ & - (a - d_{ni}) + \frac{W_{obj}}{2} + (-1)^i w = 0, \end{aligned} \tag{1}$$

where

$$\begin{aligned} O_{ix} \;=\; & (-1)^{i+1} W_{fi} + (-1)^i L_{i1} \sin\theta_{i1} \\ & + (-1)^i L_{i4} \sin(\theta_{i2} - \pi) \\ & + (-1)^i d_{fi} \cos(\theta_{i2} - \pi), \end{aligned} \tag{2}$$

$$\begin{aligned} O_{iy} \;=\; & L_{i1} \cos\theta_{i1} + L_{i4} \cos(\theta_{i2} - \pi) \\ & - d_{fi} \sin(\theta_{i2} - \pi). \end{aligned} \tag{3}$$

In contrast, since the tangential constraints are dependent on the trajectory, they are represented by nonholonomic constraints. As mentioned above, if each finger rotating inward is positive, the rolling speed of the object can be expressed as

$$\dot{s}_i = -(a - d_{ni})\{\dot{\theta}_{i2} + (-1)^i \dot{\theta}_{obj}\}. \tag{4}$$

In addition, the distance of GQ_i can be expressed as (Fig. 3):

$$GQ_i = -(x_{obj} - O_{ix}) \sin\theta_{obj} + (y_{obj} - O_{iy}) \cos\theta_{obj}. \tag{5}$$

Let d_{ti} in (6) be the tangential deformation of the i-th soft fingertip, which is parallel to the surface of the object. From (4), we can obtain the relative velocity between the object and the center of the fingertip by differentiating the equation GQ_i. Finally, we obtain the nonholonimc constraints as

$$C_i^N = G\dot{Q}_i - \dot{s}_i + \dot{d}_{ti} = 0. \tag{6}$$

These types of nonholonomic constraints are similar to constraints in steering a vehicle and are called Ptaffian constraints. Finally, we obtain four constraints.

B. Two-dimensional Model of Soft Fingertips

To calculate the lagrangian, we must first calculate the elastic potential energy of the soft fingertips. If the relative angle of the object and soft fingertip θ_{pi} is defined as

$$\theta_{pi} = \theta_{i2} + (-1)^i \theta_{obj} - \pi. \tag{7}$$

the elastic potential energy determined by the parallel distributed model [6], [7], [8] can be represented as

$$P_{fi} = \pi E\{\frac{d_n^3}{3\cos^2\theta_{pi}} + d_{ni}^2 d_{ti} \tan\theta_{pi} + d_{ni} d_{ti}^2\}, \tag{8}$$

where E denotes Young's modulus of the material of the soft fingertip. If θ_{pi} is the relative angle between the object and the fingertip, the entire elastic potential energy can be determined as

$$P_i = \pi E \sum_{i=1}^{2} \{\frac{d_n^3}{3\cos^2\theta_{pi}} + d_{ni}^2 d_{ti} \tan\theta_{pi} + d_{ni} d_{ti}^2\}. \tag{9}$$

C. Lagrangian

The Lagrangian can be derived by determining the kinetic energy, the elastic potential energy and constraints. The kinetic energy of the two 2-DOF soft fingered hand shown in Fig. 2 can be represented as a pair of parallel link mechanism manipulators. If S_{ij} is the distance between the rotational joint and the center of gravity of each link, the position of each link can be expressed as

$$x_{i1} = (-1)^{i+1} W_{fi} + (-1)^i S_{i1} \sin\theta_{i1}, \tag{10}$$
$$y_{i1} = S_{i1} \cos\theta_{i1}, \tag{11}$$
$$x_{i2} = (-1)^{i+1} W_{fi} + (-1)^i S_{i2} \sin\theta_{i2}, \tag{12}$$
$$y_{i2} = S_{i2} \cos\theta_{i2}, \tag{13}$$
$$x_{i3} = (-1)^{i+1} W_{fi} + (-1)^i L_{i2} \sin\theta_{i2} + (-1)^i S_{i3} \sin\theta_{i1}, \tag{14}$$
$$y_{i3} = L_{i2} \cos\theta_{i2} + S_{i3} \cos\theta_{i1}, \tag{15}$$
$$x_{i4} = (-1)^{i+1} W_{fi} + (-1)^i L_{i1} \sin\theta_{i1} + (-1)^i S_{i4} \sin(\theta_{i2} - \pi), \tag{16}$$
$$y_{i4} = L_{i1} \cos\theta_{i1} + S_{i4} \cos(\theta_{i2} - \pi). \tag{17}$$

Consequently, the kinetic energy of two soft fingers with a parallel link mechanism and a grasped object can be represented as

$$K = \sum_{i=1}^{2}\sum_{j=1}^{4} \frac{1}{2} m_{ij} (\dot{x_{ij}}^2 + \dot{y_{ij}}^2) + \sum_{i=1}^{2}\sum_{j=1}^{4} \frac{1}{2} I_{ij} \dot{\theta_{ij}}^2 + \frac{1}{2} m_{obj} (\dot{x_{obj}}^2 + \dot{y_{obj}}^2) + \frac{1}{2} I_{obj} \dot{\theta_{obj}}^2 \tag{18}$$

where m_{ij} is the mass and I_{ij} is the moment of inertia of each link. The angle θ_{ij} can be represented as four joint angles θ_{11}, θ_{12}, θ_{21} and θ_{22}, so $\dot{\theta_{i3}}$ and $\dot{\theta_{i4}}$ can be replaced by $\dot{\theta_{i1}}$ and $\dot{\theta_{i2}}$, respectively.

The holonomic constraint related term also needs to be added to the Lagrangean. This term is represented by Lagrange's multiplier and formula of constraint. Finally, we can obtain the Lagrangian as:

$$L = K - P_i + \sum_{i=1}^{2} \lambda_i^H C_i^H, \tag{19}$$

where λ_1^H and λ_2^H represent Lagrange multipliers corresponding to the holonomic constraints C_1^H and C_2^H. The vector $\boldsymbol{\lambda}^N = [\lambda_1^H, \lambda_2^H]^T$ is referred to as the holonomic constraint force vector.

D. Equations of Motion

In the equations, each q_j corresponds to each parameter. $\boldsymbol{q}$ is a vector of parameter q_j, which is expressed as $\boldsymbol{q} = [x_{obj}, y_{obj}, \theta_{obj}, \theta_{11}, \theta_{12}, \theta_{21}, \theta_{22}, d_{n1}, d_{n2}, d_{t1}, d_{t2}]^T$. Adding the nonholonomic constraints, we can obtain the equations of motion of soft fingered manipulation as:

$$\frac{d}{dt}\frac{\partial L}{\partial \dot{\boldsymbol{q}}_j} - \frac{\partial L}{\partial \boldsymbol{q}_j} = \boldsymbol{\Phi}^{NT} \boldsymbol{\lambda}^N \in \boldsymbol{R}^{11\times 1}. \tag{20}$$

We defined $\boldsymbol{\Phi}^{NT}$ as a partially differentiated constraint matrix of the nonholonomic constraint. This is expressed as

$$\boldsymbol{\Phi}^{NT} = \frac{\partial C_i^N}{\partial \dot{\boldsymbol{q}}_j}. \tag{21}$$

In addition, $\boldsymbol{\lambda}^N = [\lambda_1^N, \lambda_2^N]$ is the nonholonomic constraint force vector applied along the object surface. That is, the nonholonomic constraint force vector is the vector of Lagrange's multiplier.

E. Construction of Simulation

The Constraint Stabilization Method (CSM) is a numerical method that can solve ordinary differential equations under geometrical constraints. We have used this method to determine the two holonomic and two nonholonomic constraints. The CSM equations for holonomic constraints and nonholonomic constraints can be expressed as

$$\ddot{\boldsymbol{C}}^H + 2\alpha\dot{\boldsymbol{C}}^H + \alpha^2 \boldsymbol{C}^H = 0 \in \boldsymbol{R}^{2\times 1}, \tag{22}$$
$$\dot{\boldsymbol{C}}^N + \beta \boldsymbol{C}^N = 0 \in \boldsymbol{R}^{2\times 1}, \tag{23}$$

where α and β denote the CSM parameters. The higher these parameters, the faster the deviation of constraints converge to zero. If $\dot{\boldsymbol{C}}^H$ and $\dot{\boldsymbol{C}}^N$ is the vector composed of equations (1) and (6), then, for the convenience of simulation, we derived (23) and (24) as

$$\boldsymbol{\Phi}^H \dot{\boldsymbol{p}} = -\boldsymbol{b}^H(\boldsymbol{q}, \boldsymbol{p}) - 2\alpha\dot{\boldsymbol{C}}^H - \alpha^2 \boldsymbol{C}^H \triangleq -\boldsymbol{\gamma}^H \tag{24}$$
$$\boldsymbol{\Phi}^N \dot{\boldsymbol{p}} = -\boldsymbol{b}^N(\boldsymbol{q}, \boldsymbol{p}) - \beta \boldsymbol{C}^N \triangleq -\boldsymbol{\gamma}^N, \tag{25}$$

where $\boldsymbol{p}$ is the velocity vector, or is time derivative of $\boldsymbol{q}$. Furthermore, if $\boldsymbol{\Phi}^H$ is the partially differentiated holonomic

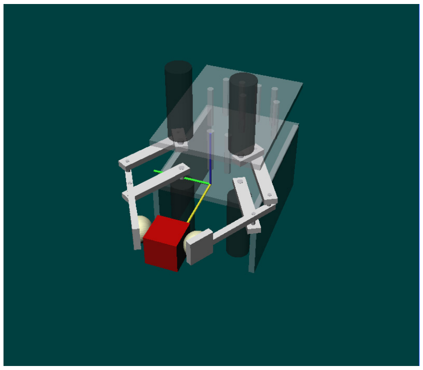

Fig. 4. Simulation of soft-fingered manipulation

constraints, then each component of vector $\boldsymbol{\Phi}^H$ corresponds to

$$\Phi_{ij}^H = \frac{\partial C_i^H}{\partial \boldsymbol{q}_j} \quad (i = 1,2 : j = 1,2,\ldots,11), \tag{26}$$

From all of the above, the matrix description of equations of motion can be expressed as:

$$\begin{bmatrix} \boldsymbol{I} & \boldsymbol{0} & \boldsymbol{0} & \boldsymbol{0} \\ \boldsymbol{0} & \boldsymbol{M} & -\boldsymbol{\Phi}^{HT} & -\boldsymbol{\Phi}^{NT} \\ \boldsymbol{0} & -\boldsymbol{\Phi}^{H} & \boldsymbol{0} & \boldsymbol{0} \\ \boldsymbol{0} & -\boldsymbol{\Phi}^{N} & \boldsymbol{0} & \boldsymbol{0} \end{bmatrix} \begin{bmatrix} \dot{\boldsymbol{q}} \\ \dot{\boldsymbol{p}} \\ \boldsymbol{\lambda}^H \\ \boldsymbol{\lambda}^N \end{bmatrix} = \begin{bmatrix} \boldsymbol{p} \\ \boldsymbol{f}_{ext} + \boldsymbol{u}_{IN} \\ \boldsymbol{\gamma}^H \\ \boldsymbol{\gamma}^N \end{bmatrix} \tag{27}$$

In this equation, $\boldsymbol{I}$ is the unit matrix, $\boldsymbol{f}_{ext}$ is the external force vector, and $\boldsymbol{u}_{IN}$ is the input vector for each rotational joint. This matrix thus includes CSM equations and equations of motion. By numerically integrating those equations, we can observe the manipulation of a soft fingered hand with parallel link mechanism. The constructed simulation is shown in Fig. 4.

III. TWO PHASED OBJECT FORCE AND COORDINATE CONTROLLER

In this section, we introduce a new control scheme for a two 2-DOF soft fingered robotic hand based on a Two Phased Object Orientation Controller.

A. Two Phased Object Orientation Controller

The softness of a soft fingertip is powerful tool in manipulation. In hard fingered manipulation, all joints of a robotic hand must be computed with Jacobian matrix. In contrast, in soft fingered manipulation, the soft material adaptively deforms against the surface of object. Consequently, even if it was imprecisely controlled, the grasped state can be maintained. A model based controller may lead to failure due to the unexpected behavior of soft fingertip. In contrast, a control without a Jacobian matrix is effective for soft fingered manipulation. In their description of a two phased posture controller, Inoue *et al.* revealed that the contact state of a soft finger and an object always converges to LMEE in manipulation [9], [10]. They also introduced a controller without a Jacobian matrix, which gradually generates the desired angle of the rotational finger joint from the equilibrium state. This new controller was successful in controlling the orientation of a grasped object with a pair of 1-DOF fingers. Their controller can be described as:

$$\theta_{fi}^d = -(-1)^i K_I \int_0^t (\theta_{obj} - \theta_{obj}^d) d\tau, \tag{28}$$

$$u_i = -K_P(\theta_{fi} - \theta_{fi}^d) - K_D\dot{\theta}_{fi} + f_{const} - f_{fvi}(\theta_{fi}). \tag{29}$$

The first stage of this controller is an integral controller, which produces the desired joint angle. The second stage of this controller is a simple PD controller. In addition, f_{const} is a controller for grasping force. In the equation, $f_{fvi}(\theta_{fi})$ is the input to negate the effect of gravity. As described above, their controller does not require a Jacobian matrix, since it was constructed with a simplified motion relationship of a soft finger and the grasped object. For example, when two fingers rotate counter clockwise, the object rotates clockwise.

B. Extension to Two Phased Object Force and Coordinates Controller

The new control scheme was designed to control the translational position of a grasped object, with orientation in a 2D plane without the force of gravity. The basic idea of the new control scheme is same as the previous scheme. In the new control scheme, the controller has two phases, the first of which produces the desired joint angle, and the second of which controls the finger using a simple PD controller. However, a higher degree of freedom of manipulation is needed to extend this idea. To enable this higher degree of freedom, it is essential to introduce other two integral controllers for producing desired angle of each joint. We therefore introduced three integral controllers:

$$\theta_x^d = K_{Ix} \int_0^t (x_{obj} - x_{obj}^d) d\tau, \tag{30}$$

$$\theta_y^d = K_{Iy} \int_0^t (y_{obj} - y_{obj}^d) d\tau, \tag{31}$$

$$\theta_\theta^d = K_{I\theta} \int_0^t (\theta_{obj} - \theta_{obj}^d) d\tau. \tag{32}$$

Furthermore, the structure of the controller should also be changed to subsume the simplified motion relationship of soft fingers and grasped object seen in the manipulation. In the equation, u_{ij} denotes the input for the two rotational joints. To enable two translation motions and one rotational motion, these simplified motion relationships should be divided into six states (Fig. 5). For example increasing u_{11} and u_{21} while decreasing u_{12} and u_{22} make the object move upward (Fig. 5-(a)). Thus, if y_{obj} is less than y_{obj}^d, we should increase u_{11} and u_{21} while decreasing u_{12} and u_{22}. In the case of Fig. 5-(b), we should decrease u_{11} and u_{21} while increasing u_{12} and u_{22}. In the case of Fig. 5-(c), we should decrease u_{11} and u_{12} while increasing u_{21} and u_{22}. In the case of Fig. 5-(d), we should increase u_{11} and u_{12} while decreasing u_{21} and u_{22}. In the case of Fig. 5-(e), hence the rotation motion of object can be achieved with only by rotating the upper most

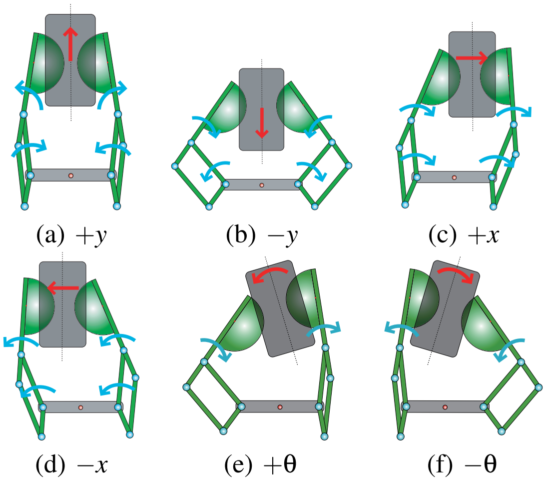

(a) $+y$ (b) $-y$ (c) $+x$

(d) $-x$ (e) $+\theta$ (f) $-\theta$

Fig. 5. Motion Relationship

joints, we should decrease u_{12} while increasing u_{22}. In the case of Fig. 5-(f), we should increase u_{12} while decreasing u_{22}. Accordingly, by putting all the term of input in each input of joint, the new control scheme can be expressed as

$$\begin{aligned} u_{11} =& -K_{Px}(\theta_{11}-\theta_{11(0)}-\theta_x^d)-K_{Dx}\dot{\theta}_{11} \\ & -K_{Py}(\theta_{11}-\theta_{21(0)}+\theta_y^d)-K_{Dy}\dot{\theta}_{11}+f_{const} \end{aligned} \tag{33}$$

$$\begin{aligned} u_{21} =& -K_{Px}(\theta_{21}-\theta_{21(0)}+\theta_x^d)-K_{Dx}\dot{\theta}_{21} \\ & -K_{Py}(\theta_{21}-\theta_{21(0)}+\theta_y^d)-K_{Dy}\dot{\theta}_{21}+f_{const} \end{aligned} \tag{34}$$

$$\begin{aligned} u_{12} =& -K_{Px}(\theta_{12}-\theta_{12(0)}-\theta_x^d)-K_{Dx}\dot{\theta}_{12} \\ & -K_{Py}(\theta_{12}-\theta_{12(0)}-\theta_y^d)-K_{Dy}\dot{\theta}_{12} \\ & -K_{P\theta}(\theta_{12}-\theta_{12(0)}-\theta_\theta^d)-K_{D\theta}\dot{\theta}_{12}+f_{const} \end{aligned} \tag{35}$$

$$\begin{aligned} u_{22} =& -K_{Px}(\theta_{22}-\theta_{22(0)}+\theta_x^d)-K_{Dx}\dot{\theta}_{22} \\ & -K_{Py}(\theta_{22}-\theta_{22(0)}-\theta_y^d)-K_{Dy}\dot{\theta}_{22} \\ & -K_{P\theta}(\theta_{22}-\theta_{22(0)}+\theta_\theta^d)-K_{D\theta}\dot{\theta}_{22}+f_{const} \end{aligned} \tag{36}$$

In this new controller, all rotational joints act to control two axial translational positions of the grasped object. In contrast, only the two uppermost rotational joints act to control the object posture. Since a parallel link mechanism has a singular point, joint angles are limited. For example, the initial angle of each joint was not zero, so the incipient inputs can be extremely high. To eliminate the possibility of these excessive inputs, we added $\theta_{ij(0)}$, which denotes the initial angle of each joint in the controllers.

IV. SIMULATION OF OBJECT POSTURE AND POSITION CONTROL

We simulated manipulations performed by a soft fingered hand consisting of two fingers, each with 2-DOFs, in the absence of the force of gravity, to assess the validity of proposed control scheme. In the simulation, position control and orientation control were simulated. Physical parameters, parameters of simulation and control gains are shown in TABLE I, II and III, respectively. All the parameters in TABLE I are based on those of actual soft fingered hands. If

TABLE I

PHYSICAL PARAMETERS

Parameters	Value
m_{obj}	0.1 kg
I_{obj}	41.7 kg·mm^2
W_{obj}	50 mm
$2W_{fi}$	100 mm
d_{fi}	5 mm
$L_{11}, L_{21}, L_{13}, L_{23}, L_{14}, L_{24}$	100 mm
L_{12}, L_{22}	30 mm
S_{11}, S_{21}	4.9 mm
S_{12}, S_{22}	1.4 mm
S_{13}, S_{23}	4.5 mm
S_{14}, S_{24}	5.7 mm
m_{11}, m_{21}	66 g
m_{12}, m_{22}	28 g
m_{13}, m_{23}	73 g
m_{14}, m_{24}	113 g
I_{11}, I_{21}	224.5 kg·mm^2
I_{12}, I_{22}	13.6 kg·mm^2
I_{13}, I_{23}	233.5 kg·mm^2
I_{14}, I_{24}	672.7 kg·mm^2
Viscosity for d_{ni}	400Ns/m
Viscosity for d_{ti}	400Ns/m
E Young's modulus	0.232MPa

TABLE II

PARAMETERS OF SIMULATION

Parameters	Value
Sampling time	0.1msec
α	20000
β	10000

the point of origin is the initial position of a grasped object, the sequence of control can be expressed as:

1) Initial state:Two fingers start grasping
2) Operation 1:$(x^d_{obj}, y^d_{obj}, \theta^d_{obj}) = (20\text{ mm}, 0, 0)$
3) Operation 2:$(x^d_{obj}, y^d_{obj}, \theta^d_{obj}) = (0, 0, 0)$
4) Operation 3:$(x^d_{obj}, y^d_{obj}, \theta^d_{obj}) = (-20\text{ mm}, 0, 0)$
5) Operation 4:$(x^d_{obj}, y^d_{obj}, \theta^d_{obj}) = (0, 0, 0)$
6) Operation 5:$(x^d_{obj}, y^d_{obj}, \theta^d_{obj}) = (0, 20\text{ mm}, 0)$
7) Operation 6:$(x^d_{obj}, y^d_{obj}, \theta^d_{obj}) = (0, 0, 0)$
8) Operation 7:$(x^d_{obj}, y^d_{obj}, \theta^d_{obj}) = (0, -20\text{ mm}, 0)$
9) Operation 8:$(x^d_{obj}, y^d_{obj}, \theta^d_{obj}) = (0, 0, 0)$
10) Operation 9:$(x^d_{obj}, y^d_{obj}, \theta^d_{obj}) = (0, 0, 10\text{ deg})$
11) Operation 10:$(x^d_{obj}, y^d_{obj}, \theta^d_{obj}) = (0, 0, 0)$
12) Operation 11:$(x^d_{obj}, y^d_{obj}, \theta^d_{obj}) = (0, 0, -10\text{ deg})$

Graphs of the simulation results show that these simulation results converge to the desired position or orientation (Fig. 6). The contact state converges to an equilibrium, which is uniquely decided by the position of the fingertips and the object. Furthermore, two fingers adaptively change their joint angle to match the current coordinates of the grasped object. Consequently, an object controlled by a non Jacobian controller can be coordinated precisely by adaptively deciding the finger joint angles based on the LMEE. These findings indicate the validity of the proposed controller in controlling object planar coordinates.

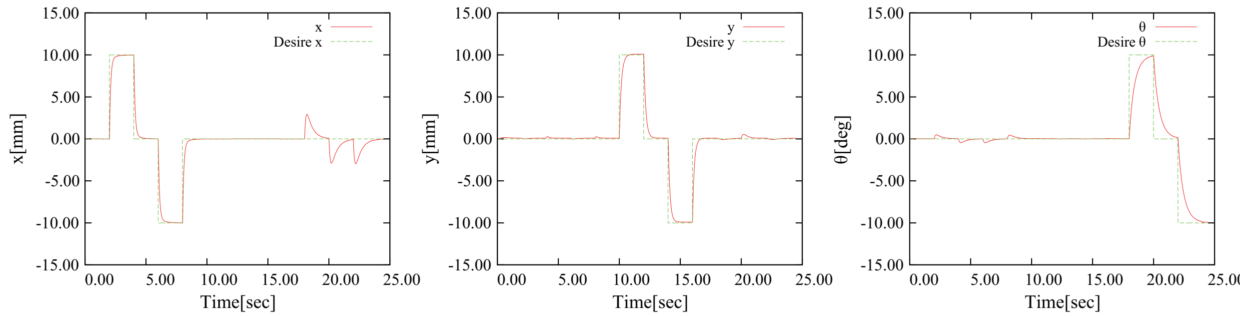

(a) x_{obj} vs. time (b) y_{obj} vs. time (c) θ_{obj} vs. time

Fig. 6. Simulation result of object position and posture control

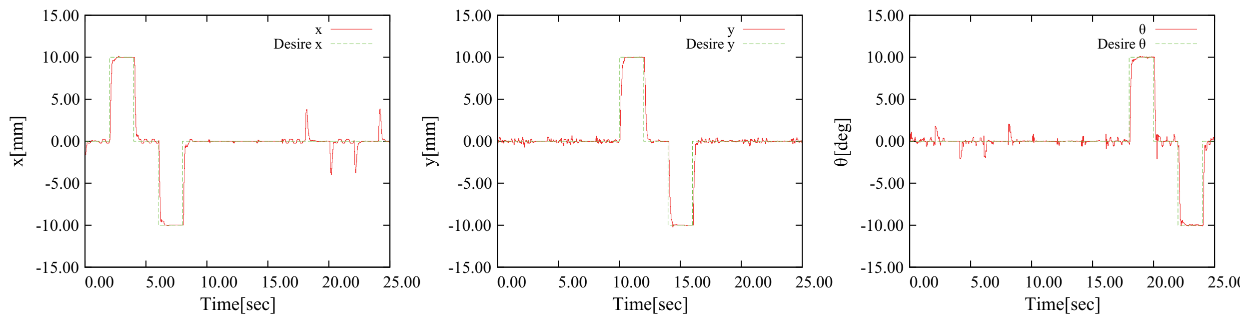

(a) x_{obj} vs. time (b) y_{obj} vs. time (c) θ_{obj} vs. time

Fig. 7. Experiment result of object position and posture control

TABLE III
CONTROL GAINS

Parameters	Value
Sampling time of object coordinates data	30msec
K_{Px} gain	70
K_{Py} gain	70
$K_{P\theta}$ gain	20
K_{Dx} gain	20
K_{Dy} gain	20
$K_{D\theta}$ gain	20
K_{Ix} gain	0.1
K_{Iy} gain	0.1
$K_{I\theta}$ gain	0.02
f_{const}	2 Nm

V. EXPERIMENT OF OBJECT POSTURE AND POSITION CONTROL

The same manipulation as the previous simulation was performed by an actual soft fingered hand. Gains of controller were set as shown in TABLE III. The control order was the same as in the simulation. Experimental results are shown in Fig. 7. As in the simulation, we observed the convergence of the results to the desired values. These convergences were faster than during the simulation. Even in an actual soft fingered manipulation, the proposed controller can work precisely.

TABLE IV
FORCE CONTROL GAINS

Parameters	Value
K_{Pf} gain	70
K_{Df} gain	0
K_{Df} gain	0.1

VI. SIMULATION OF OBJECT FORCE AND COORDINATES CONTROL

Our controller is an independent controller of grasping force, indicating that control of grasping force and object coordinates can occur simultaneously. To assess the behavior of this controller, we attempted to control the grasping force and coordinate control simultaneously. We therefore introduced a grasping force controller to the object posture position controller. This new controller can be expressed by replacing the f_{const} terms of (34), (35), (36), (37) with the controller below:

$$f_{grasp} = -K_{Pf}\left\{\theta_{ij} - \theta_{ij(0)} + K_{If}\int_0^t (f_n - f_n^d)d\tau\right\} - K_{Df}\dot{\theta}_{ij}. \tag{37}$$

Let f_n be the feed back of normal reaction force of object surface, let f_n^d be the desired grasping force. The parameters of grasping force controller is shown in TABLE IV.

In this simulation, we used the reaction force that arises to a fingertip for force feedback. The parameters and control sequence were identical to those of the previous simulation.

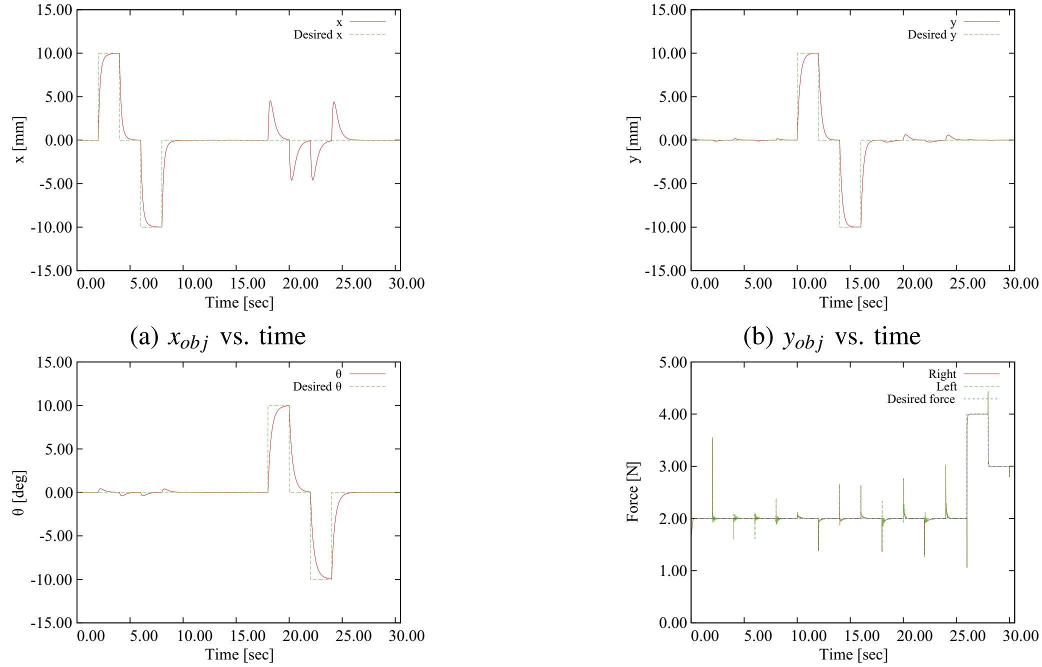

(a) x_{obj} vs. time
(b) y_{obj} vs. time
(c) θ_{obj} vs. time
(c) f_n vs. time

Fig. 8. Simulation result of object force and coordinates control

However, adding force controller slows down the controller of orientation controller. Hence, we changed the gain of orientation controller as $K_{I\theta} = 0.04$. Furthermore, additional operations were added:

1) Initial state:Two fingers start grasping
2) Operation 1-11:$f_n^d = 2\ N$
3) Operation 12:$(x_{obj}^d, y_{obj}^d, \theta_{obj}^d, f_n^d) = (0, 0, 0, 4\ N)$
4) Operation 13:$(x_{obj}^d, y_{obj}^d, \theta_{obj}^d, f_n^d) = (0, 0, 0, 3\ N)$

The results of simulation are shown in Fig. 8. There were no big difference in x_{obj}, y_{obj} and θ_{obj} between these results and those of the previous simulation. Furthermore, grasping forces converge quickly to the desired force because of grasping force's short sampling time compared with the sampling time of object's coordinate. These findings indicate that this proposed controller can simultaneously control the grasping force and the object's three coordinates. Although there were some spikes in grasping force, they are just noise caused by CSM. These spikes will not happen with the experiment. That is to say, these spikes can be explained with the artifact caused by CSM. As long as the equations of constraint are zero, CSM does not generate large forces to maintain the constraints. However, once the balance is broken, CSM generate the forces and cause fast convergence to the balanced state. Thereby, viscosity of soft fingertips reacts with large forces. As shown in Fig. 8, those spikes can be seen at some points where the constraints tend to lose their balance. Reducing the viscosity of soft fingertips can make these spikes smaller.

VII. CONCLUSION

We have described a two phased controller for a pair of 2-DOF soft fingers, which can control an object's three coordinates. Furthermore, we applied a grasping force controller to proposed controller. In all simulations and experiments, the results followed the desired trajectory. We confirmed the validity of this controller, both through simulations and experiments. However, in the last simulation we only dealt with the grasped object being a cube. Changing the shape of the object may alter the result, indicating the need for further investigation of grasping force control.

REFERENCES

[1] H.Hanafusa and H.Asada, "Stable Prehension by a Robot Hand with Elastic Fingers", *Proc. 7th Int. Symp. Industrial Robots,* pp.361-368, 1977.
[2] H.Hanafusa and H.Asada, "A robot Hand with Elastic Fingers and Its Application to Assembly Process", *IFAC Symp. Information and Control Problems in Manufacturing Technology*, pp. 127-138, 1977.
[3] S.Arimoto, P.Nguyen, H.Y.Han, and Z.Doulgeri, "Dynamics and control of a set of Dual Fingers with Soft Tips", *Robotica*, Vol.18, pp.71-80, 2000.
[4] Z.Doulgeri, H.Fasoulas and S.Ariomoto, "Feedback Control for Object Manipulationi by a pair of Soft Tips", *Robotica*, Vol.20, pp.1-11, 2002.
[5] Z.Doulgeri, H.Fasoulas, "Grasping Control of Rolling Manipulation with Deformable Fingertips", *IEEE/ASME Trans. Robotics*, Vol.22, No.6, pp.1273-1279, 2006.
[6] T.Inoue and S.Hirai, "Local Minimum of Elastic Potential Energy on Hemispherical Soft Fingertip", *IEEE Int. Conf, Robotics and Automation*, 2005.
[7] T.Inoue and S.Hirai, "Dynamic Stable Manipulation via Soft-fingered Hand", *IEEE Int. Conf. Robotics and Automation*, 2007.
[8] T.Inoue and S.Hirai, "Study on Hemispherical Soft-Fingered Handling for Fine Manipulation by Minimum D.O.F Robotic Hand", *IEEE Int. Conf. Robotics and Automation*, 2006.
[9] T.Inoue and S.Hirai, "A Two-Phased Object Orientation Controller on Soft Finger Operation", *IEEE/RSJ Int. Conf. Intelligent Robots and Systems*, 2007.
[10] T.Inoue and S.Hirai, "Two-stage Control via Virtual Desired Values in Soft-fingered Manipulation with Time Delay", *IEEE Int. Conf. Robotics and Biomimetics*, 2007.